Chapter 8

Hydrated Electron Clusters

8.1 Introduction

The hydrated electron plays an important role in many areas of condensed-phase science such as radiation physics, biological activity, electron transfer, and charge-induced reactivity. However, a molecular level understanding of electron solvation, knowledge of which is fundamental to the understanding of basic solute-solvent phenomena, is far from complete. First evidence for the hydrated electron was found in 1962 by Hart and Boag [13] who observed a transient broad absorption band peaking at 720 nm after irradiation of pure liquid water with an electron pulse and assigned it to hydrated electrons.

Structural information on the hydrated electron was initially obtained by electron spin resonance of electrons in 10 M sodium hydroxide aqueous glass [265]. This study indicated that the electron is surrounded by six water molecules, each singly hydrogen-bound to the electron, in an octahedral configuration. However, it has to be noticed that an 10 M solution of NaOH amounts to $\sim$5 H_2O per Na^+ and OH^-, which suggests that hydrated electrons in neat water may very well behave differently. Interestingly, the electron spin-echo patterns were later reinterpreted [266] and attributed to just two protons of a single dipole-oriented water molecule in the first solvation shell. More evidence for an octahedral configuration came from molecular dynamics simulations [267], which successfully captured most aspects of transient absorption spectra of solvated electrons. More recent resonance Raman studies on aqueous solvated electrons supported the original octahedral model, in which the nearest neighbor water molecules form a strong hydrogen bond with the electron via a single proton, as evidenced by strongly enhanced, and moderately red-shifted intramolecular bending and blue-shifted libration modes [268–270] compared to bulk water.

Finite water clusters have drawn considerable attention, as they represent potential model systems for characterizing the water network accommodating the excess elec-

tron under well controlled conditions and as a function of size. $(H_2O)_n^-$ clusters were first detected in mass spectroscopy experiments by Haberland and coworkers [271]. Structural information from experiments and calculations on isolated hydrated electron clusters has, however, remained controversial, as well as the critical size beyond which the cluster anions resemble the bulk hydrated electron.

In early molecular dynamics simulations [15–18] the interaction of the assumed rigid water molecules among themselves is treated classically, while quantum mechanics is used to describe the electron–molecule interaction. They found that electron localization on the cluster surface is more stable for smaller clusters ($n \leq 32$), while internally solvated electron is the stable configuration for larger clusters ($n \geq 64$). Electron vertical detachment energies (VDE), which correspond to the minimum amount of energy required to remove the electron from the cluster anion with no molecular rearrangement, were predicted to be considerably lower for the surface states than for the internal states. Thus, photoelectron spectroscopy of $(H_2O)_n^-$ clusters should yield the size at which the surface-to-internal structural transformation occurs. Instead, photoelectron spectroscopy of negatively charged water clusters found evidence for (at least) three isomeric classes, I to III, characterized by different VDE, which coexist and evolve smoothly over a broad range of cluster sizes [19–22]. The presence and coexistence of different isomers against theoretical predictions can possibly be rationalized considering the absence of thermal equilibrium of the ion population produced in beam sources. One can thus assume isomers II and III to be metastable. However, another inconsistency between theory and experiments was pointed out as VDE was extrapolated to infinite cluster sizes (bulk water). If r is the (van der Waals) radius of an atom or molecule and R the radius of a spherical cluster containing n atoms, the cluster's volume is given by $V = 4\pi R^3 = n4\pi r^3$. Thus, $n = (R/r)^3$, or $n^{-1/3} = 1/(R/r)$. From an electrostatic calculation [18] for the energy to eject an electron from the center of a homogeneous dielectric sphere one obtains:

$$\mathrm{VDE}(n) = \mathrm{VDE}(n = \infty) - \frac{e^2}{2\,r}\left(1 + \frac{1}{D_{\mathrm{opt}}} - \frac{1}{D_{\mathrm{stat}}}\right)n^{-1/3}, \tag{8.1}$$

where D_{opt} and D_{stat} are the optical and static dielectric constants of water. Equation (8.1) says, that a straight line is expected for the VDE on a $n^{-1/3}$ plot if electrostatic effects prevail and if the electron is in an interior state inside the cluster. Except for the small water cluster size ($n < 7$), VDE from photoelectron spectra [19–22] for isomer I can be very well fit by a straight line and inserting the known values into equation (8.1) one finds a surprisingly good agreement with the experiment for water. Furthermore, extrapolation of the vertical binding energies to infinite size (the bulk) yielded a value of 3.3 eV, which is close to the photoelectric threshold of water, 3.2 eV [19]. However, the measured vertical binding energies, are in good agreement with the values simulated for the surface states [16] (whereas calculated values for internal states extrapolate to 5.1 eV). A similar inconsistency—i.e. extrapolation of

experimental data to bulk values supporting internal solvation that are found to be in good agreement with calculations for surface states—was found in electronic absorption spectra of $(H_2O)_n^-$ ($15 \leq n \leq 50$) measured by Ayotte and Johnson [26]. Further experimental support for the existence of internally solvated structures already at small cluster sizes comes from time-resolved experiments [272, 273].

In 1994, Makov and Nitzan [274] showed that the free energy of transfer for an electron between the surface and the interior of a spherical water cluster essentially vanishes, using a continuum dielectric model. In addition, they showed that both interior and surface states manifest the linear scaling of the VDE with $n^{-1/3}$, so that scaling did not distinguish the excess electron-binding morphologies. Therefore, for the infinite cluster, both surface and interior states must extrapolate to the same bulk limit. Hence, the experimental observation of an extrapolated value close to the bulk does not a priori distinguish between surface and interior states [275]. In 2001, analyzing Ayotte and Johnson's electronic absorption spectra [26], Bartels [276] claimed that the model potential used for the simulation binds the electron too tightly. Hence, simulations overestimated VDEs of interior states. In 2005, Rossky and coworkers [275] calculated that clusters in the range n=20–200 support stable surface states, which are compatible both with the experimental data and their extrapolation to bulk, and suggested that the transition to an interior state should occur for larger clusters than observed to date. Recent ab initio studies [277,278], however, did find internally-solvated structures for clusters as small as $(H_2O)_{14}^-$, calling again into question the ability of the water pseudo-potentials employed in the quantum simulations to correctly describe the properties of the diffuse electron as well as the many-body interactions in water.

More detailed insight into the structure and binding in hydrated electron clusters comes from the IR-PD studies by Johnson and coworkers [27–30]. Vibrational action spectra of bare $(H_2O)_n^-$ clusters were measured in the OH stretching region up to n=21, but the n>9 spectra suffered from lifetime broadening [29]. Vibrational predissociation spectra of bare (n=15) and Ar-tagged (n=3–24) hydrated electron clusters were also measured in the water bending region, establishing the double H-bond acceptor (AA) motif for small- and medium-sized (n<24) type I clusters [30]. The AA-motif is characterized by a uniquely red-shifted bending band in the 1500–1550 cm^{-1} region, due to significant charge transfer into the O−H σ^* orbitals [279]. The more weakly binding type II clusters do not display the AA feature [280], but instead contribute broad structures at intermediate redshifts. These results raise the interesting question of whether the AA-motif is specific to smaller clusters or if it persists in larger clusters and possibly in the bulk phase, as originally indicated by Dikanov and Tsvetkov [266]. Moreover, these studies suggest that a classification of the isomer classes based on the nature of the local binding site of the hydrated electron rather than the original concept of internal vs. surface hydration may be more useful, at least for smaller clusters [280].

Here, the IR-PD spectra of the $(H_2O)_n^-$ clusters ranging from n=15 up to n=50 are

presented. They are measured in the water bending and, for the first time, librational region of the spectrum, directly addressing the question of the AA motif. The ions are "adiabatically" cooled through many collisions with He-atoms, substantially reducing the complexity, compared to previous experiments, introduced by the production of kinetically-trapped metastable isomers [21].

8.2 Experimental Details

Water cluster anions are generated by passing 2 bar of argon over H_2O prior to supersonic expansion into a vacuum through the high-temperature Even-Lavie pulsed valve at a 100-Hz repetition rate. Ions are thermalized in the trap for at least 50 ms before FELIX fires. All here presented spectra are measured by recording the depletion of the species under investigation in dependence on FELIX wavelength.

8.3 Results and Discussion

IR-PD spectra of the hydrated electron clusters $(H_2O)_n^-$ are measured for cluster sizes from n=15 to 50. Smaller sizes are difficult to trap due to electron autodetachment upon collisions with the He buffer gas in the trap. The largest cluster measured approached the upper mass-limit of the quadrupole mass filter. Representative overview IR-PD spectra for three $(H_2O)_n^-$ clusters (n=16, 20 and 45) are shown in Figure 8.1. The normalized depletion signal of the parent anion is plotted in the range from 580 to 1800 cm^{-1}. In the n=16 spectrum three absorption features, labeled A to C in Figure 8.1, are observed: a weak and broad feature at ∼700 cm^{-1} (A) and two more narrow and intense bands at 1520 (B) and 1620 cm^{-1} (C). The relative intensities and widths of these bands change with cluster size. For the smaller clusters the most prominent feature is band C, followed by band B and then A. Band B looses in intensity relative to C and A with increasing cluster size. Band C broadens considerably with increasing cluster size, while band A remains similar in shape and becomes the most prominent feature in the spectra of the larger clusters. The relative areas of bands A and C roughly scale with the number of water molecules, while band B clearly does not.

Bands B and C for $(H_2O)_{16}^-$ in Figure 8.1 match those seen previously for bare $(H_2O)_{15}^-$ by Johnson and coworkers [30]. Both bands are assigned to water bending modes; the higher frequency band (band C in Figure 8.1) is attributed to water molecules interacting only weakly with the extra electron, while the strongly redshifted band (band B in Figure 8.1) is assigned to the single double H-bond acceptor (AA) water molecule, the binding site of the excess electron. The unstructured band A has not been observed before in the gas phase, but is known from condensed phase

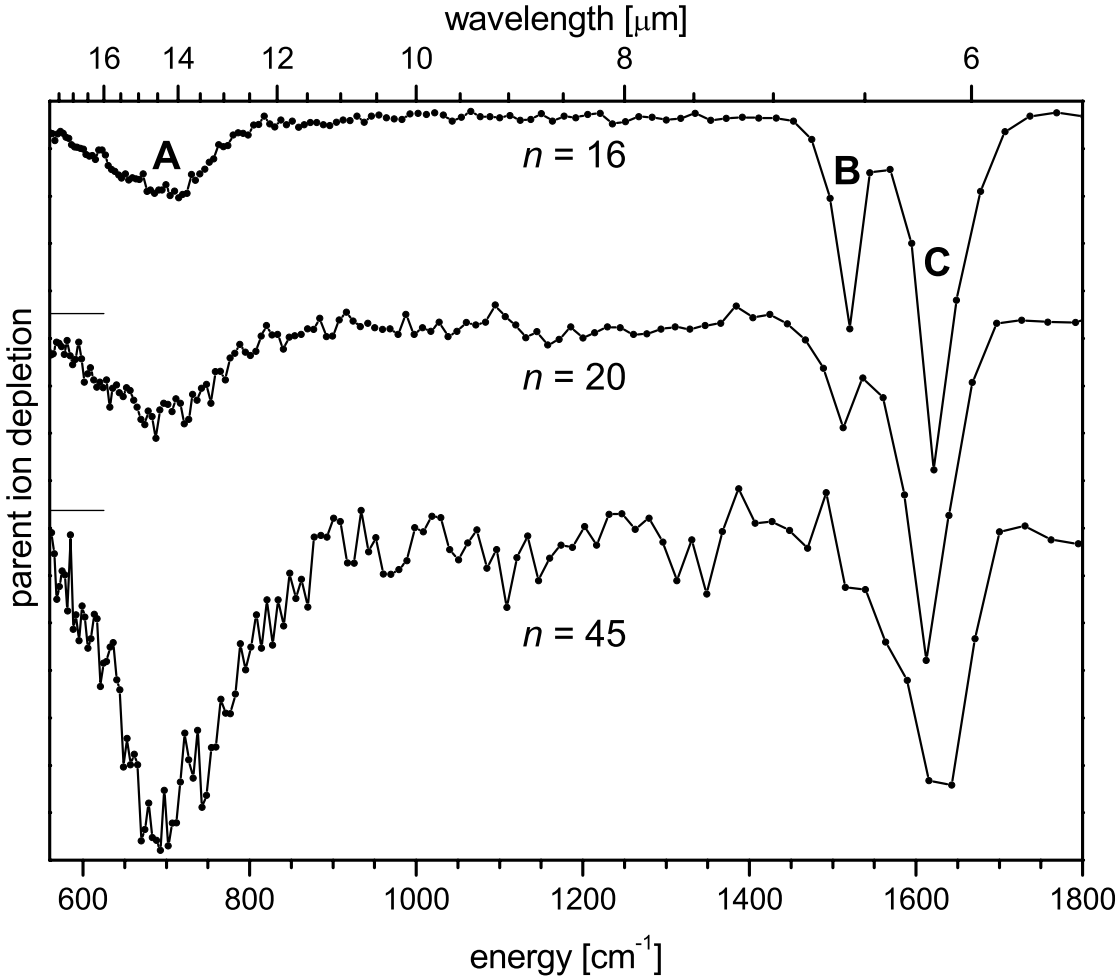

Figure 8.1: Overview IR-PD spectra of the $(H_2O)_n^-$ clusters n=16, 20 and 45 in the region from 660 to 1800 cm^{-1}. The parent yield is plotted as a function of the irradiation wavelength (top axis) and corresponding photon energy (bottom axis). The individual spectra have been normalized to the strongest depletion feature in each spectrum. The three main depletion features are labeled A, B, and C, respectively.

spectra and is assigned to water librational modes. It lies close to the corresponding band observed at 685 cm^{-1} in liquid water (at 273 K) [260] and somewhat further from the ∼800 cm^{-1} librational band in polycrystalline ice (at 266 K) [281]. A similarly broad band is observed at 698 cm^{-1} in the room temperature resonance Raman spectrum of the hydrated electron [270].

In order to look at the evolution of the position and contour of the water libration and bending bands with cluster size in more detail, IR-PD spectra are measured with

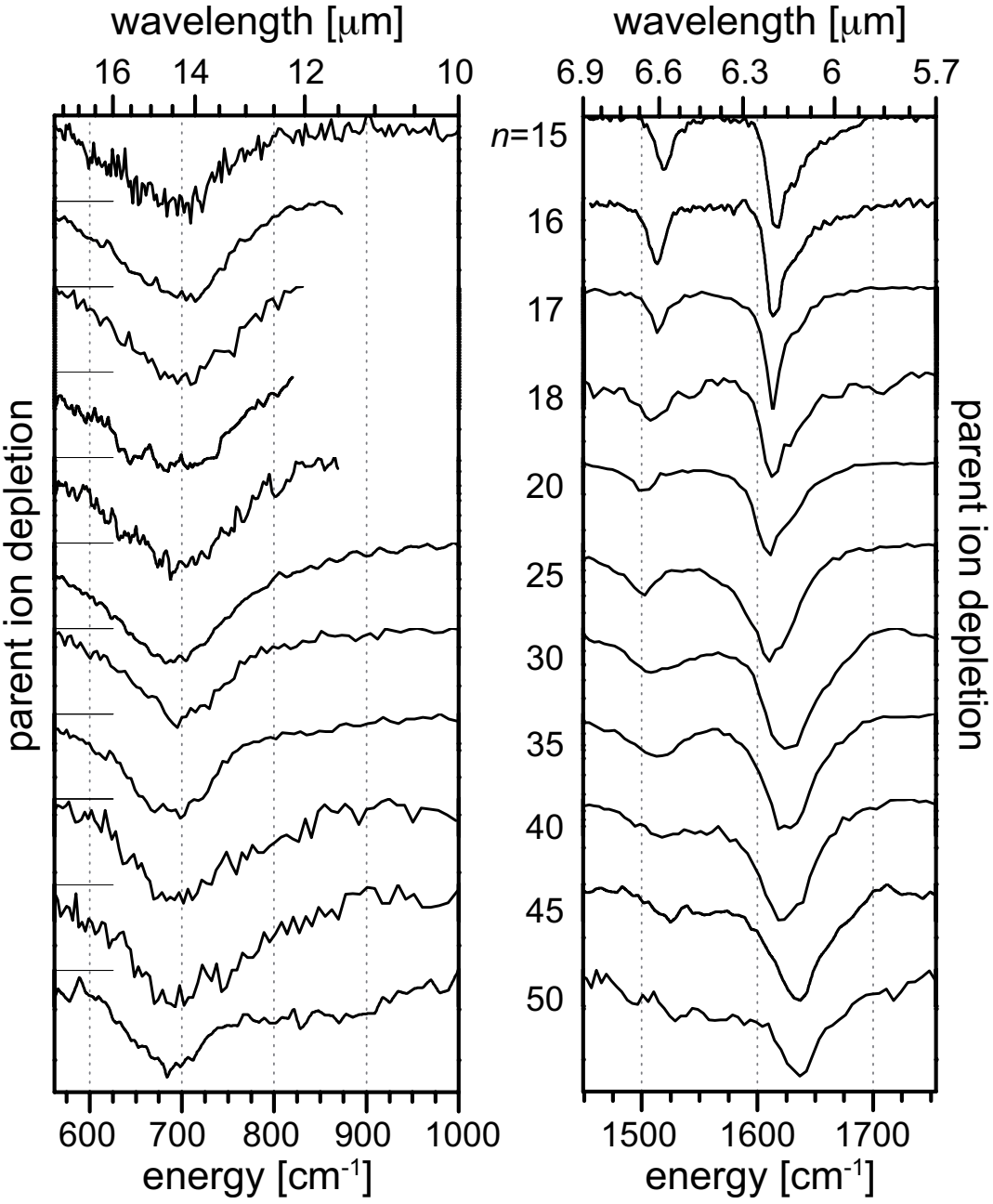

Figure 8.2: Higher resolution IR-PD spectra of the $(H_2O)_n^-$ clusters ranging from n=15 to 50, in the region of the water librational modes (560–1000 cm^{-1}) and the water bending mode (1450–1755 cm^{-1}). The parent ion yield is plotted as a function of the irradiation wavelength (top axis) and corresponding photon energy (bottom axis). Each spectrum has been normalized to its strongest depletion feature.

smaller step sizes and longer acquisition times. These IR-PD spectra, obtained for cluster sizes ranging from n=15 to 50 are shown in Figure 8.2 and band maxima are plotted in Figure 8.3. The spectra are normalized to the most intense feature in each individual spectrum. Information on the hydrogen bonding network can be extracted from the spectra measured in the water librational region (550–1000 cm^{-1}). In the n=15 spectrum band A extends from 570 to 800 cm^{-1}, with an absorption maximum at ∼710 cm^{-1}. The width of this band increases considerably with cluster size, in particular to shorter wavelengths, while its absorption maximum gradually moves to longer wavelengths, suggesting a weakening of the hydrogen bonding network on average, and is found at 683 cm^{-1} in n=50, close to the value found for liquid water. Overall, it shows the smallest dependence on cluster size of the three bands.

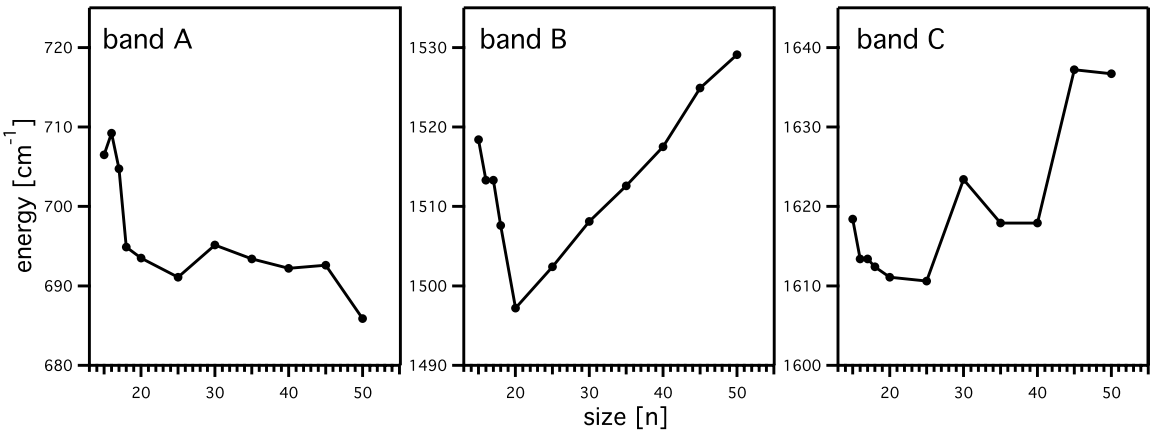

Figure 8.3: Peak positions for the three observed absorption bands, A, B, and C, in dependence on the cluster size (n).

Band C, found at 1618 cm^{-1} in the n=15 spectrum, is rather broad, extending from ∼1590 to 1700 cm^{-1}, and has a pronounced asymmetric shape. From a comparison to the calculated and experimental spectra of smaller water cluster,e.g. $(H_2O)_6^-$ and $(H_2O)_8^-$ [280,282], the asymmetric shape can be traced back to be the result of multiple bending modes of water molecules in slightly different hydrogen-bonded environments. Band C broadens with increasing cluster size. Interestingly, its peak position remains at ∼1610 cm^{-1} until n=25, close to the band maximum found in the Raman spectrum of solvated electrons (1609 cm^{-1}) [270]. For larger clusters this band monotonically shifts to higher frequencies, up to 1637 cm^{-1} in n=50, close to the value of the water bending band in ice (1630 cm^{-1}) [281] and in liquid water (1640 cm^{-1}) [270], suggesting that the band position has converged to the value of bulk water. For comparison, the bend mode of gas phase H_2O lies at 1595 cm^{-1}.

Band B, in the spectral region between 1450 and 1600 cm^{-1}, is particularly interesting, as it reflects the water bending motion of molecules interacting more strongly

with the excess electron. Band B monotonically red-shifts from 1518 cm^{-1} in n=15 to 1497 cm^{-1} in n=20. Between n=25 and 35, band B broadens and its maximum exhibits a small but distinct blue-shift of 15 cm^{-1}, and a new feature emerges between the maxima of band B and C. Above n=35, band B has largely evolved into a broad absorption in the 1475–1600 cm^{-1} region. The minimum observed in the vibrational frequency of band B between n=20 and n=25 indicates that charge transfer of electron density into the σ^* orbital of the unique AA water molecule is the largest at this point. The subsequent blue-shifting and broadening suggests that the excess electron is beginning to interact directly with multiple water molecules. Interestingly, some intensity remains at 1500 cm^{-1} even at n=50, indicating that the original AA motif observed in the smaller clusters contributes also at larger cluster sizes, but the electron is now also interacting strongly with other water molecules, similar to results seen for smaller type II cluster anions [280].

By n=50 the bend and librational peaks have essentially converged to those of liquid water, with the main signature of the electron being the broad component of the bend band. However, at an estimated ion internal temperature of close to 20 K the hydrated electron clusters are not liquid and the question arises, why the n=50 spectrum in the region of the librational modes resembles that of liquid water more than that of ice. This observation is attributed to the finite size of the cluster examined here. In neutral water clusters the onset of crystallinity occurs somewhere in-between 200 to 1000 water molecules [283], i.e., at much larger cluster sizes than probed here. Smaller water clusters correspond to quasi spherical nanoparticles with a crystal interior and a disordered "reconstructed" surface [284], as a result of their tendency to minimize dangling bonds, while even smaller clusters contain only "surface" water molecules. The reconstruction of the cluster surface leads to a weakening of the hydrogen bonding network and thus a red shift of the librational band in the present IR-PD spectra compared to the IR spectrum of bulk ice.

In Figure 8.4, the present data for n=45 is plotted together with the resonance-enhanced Raman spectrum of hydrated electrons in aqueous solution of Tauber and Mathies [270]. Care has to be taken in comparing the two types of spectra. The resonance-enhanced signal in the Raman spectra is due mainly to vibrational modes that couple strongly to the electronic excitation of the confined electron, while the IR-PD spectra behave more like IR absorption spectra in that they reflect all IR-active modes of the cluster. However, it is still interesting to note that the two types of spectra agree surprisingly well. The maximum of the water bending band in the resonance Raman spectrum lies in-between the maxima of bands B and C, i.e., where the broad feature lies that we attribute to the interaction of the electron with multiple water molecules. Interestingly, this Raman band extends down to 1400 cm^{-1} and shows substantial signal in the 1400–1550 cm^{-1} region. This region is specific to the AA-binding motif in the IR-PD spectra of the clusters, lending support to the idea that this motif may be important also in the bulk.

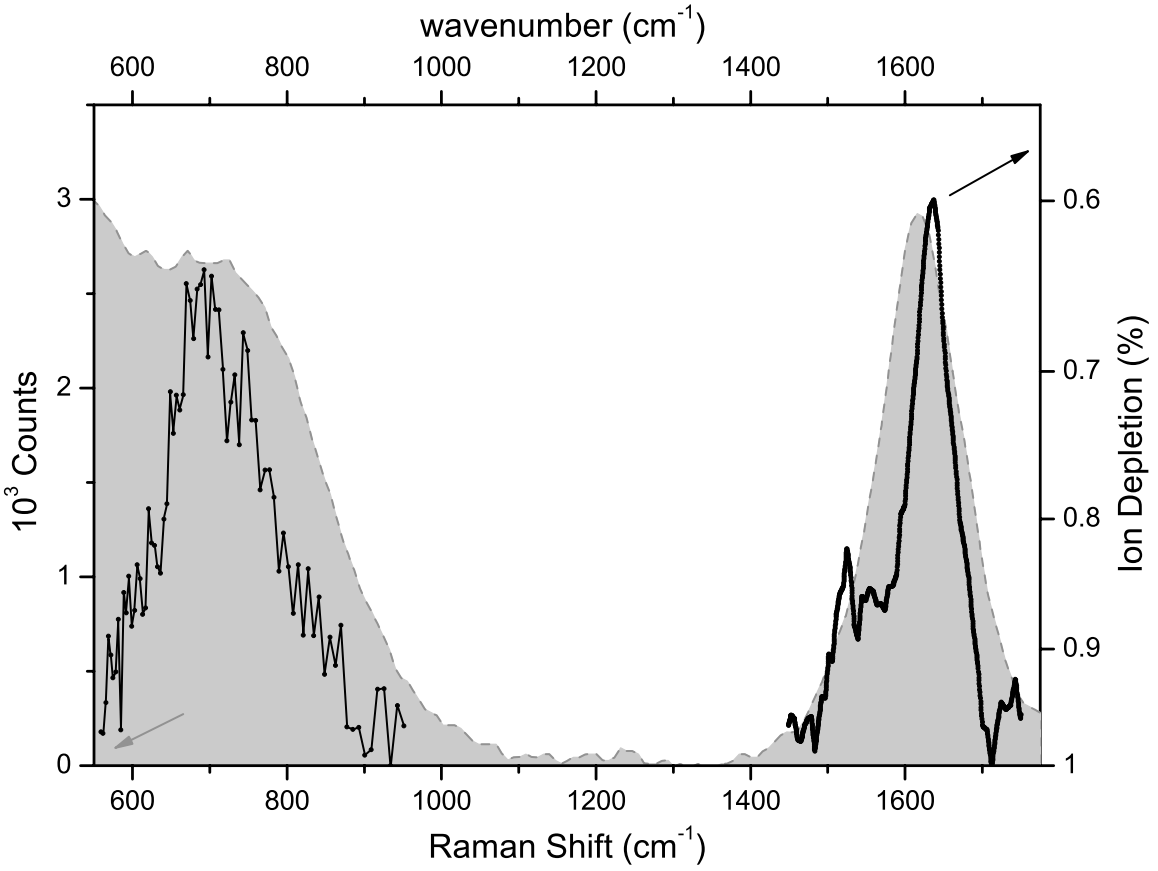

Figure 8.4: Comparison of the resonance-enhanced Raman spectrum of aqueous solvated electrons (gray broken line, gray shaded, from Ref. [270]) to the (higer resolution) IR-PD spectra of $(H_2O)_n^-$ (black line with dots) in the region from 550 to 1775 cm^{-1}.

In order to gain some insight into the nature of the isomer(s) probed in the present experiment, the IR-PD spectrum of n=15 (spectrum A in Figure 8.5) is compared to the spectra measured by Johnson and coworkers [30] of bare $(H_2O)_{15}^-$ and $(H_2O)_{15}^-$·Ar, measured using a table-top OPO/OPA laser system. In that study, the isomer distributions in the ion ensembles were determined with photoelectron spectroscopy, finding that the bare cluster was prepared exclusively as isomer I, while I and II both contributed to the Ar-tagged species. Good agreement is found between the two IR spectra of bare $(H_2O)_{15}^-$, clearly indicating that the same isomeric class, i.e. isomer I, is probed in both experiments. The bands in the present spectra are somewhat narrower, despite the 4–5 times larger bandwidth of the FEL radiation, reflecting a considerable lower ion temperature in the present experiment (∼20 K vs. <130 K). Interestingly, the Ar-tagged spectrum (C) is blue-shifted, broader and displays an additional shoul-

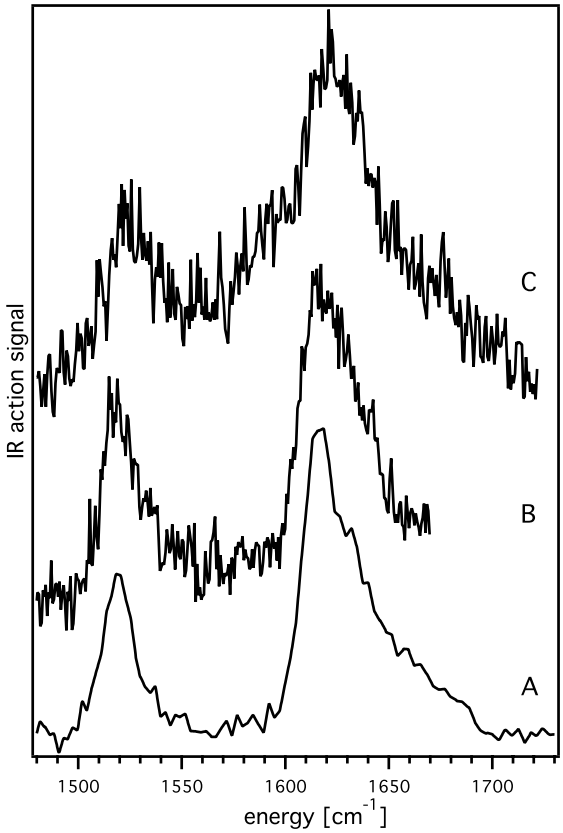

Figure 8.5: Comparison if the IR-PD spectrum of bare $(H_2O)_{15}^-$, labeled A (present study), to the spectra of "hot" bare $(H_2O)_{15}^-$ (B) and of $(H_2O)_{15}^-$·Ar (C) from Johnson and coworkers [30].

der at 1590 cm^{-1}, consistent with expectations for the spectra of mixed ensemble of isomers I and II. In particular, the shoulder likely results from a kinetically-trapped higher-energy structure (II), which is clearly not present in the IR-PD spectrum of the collisionally cooled ions in the present experiment.

8.4 Summary

From this study it appears that the electron binding in the clusters up to n=20–25 is dominated by the AA-binding motif, i.e., binding to predominantly a single water molecule, which is dipole-oriented and points its two hydrogen atoms into the electron cloud. Starting in-between n=20 and n=25 other water molecules directly interact with the additional electron, suggesting the start of formation of a cavity near the surface of the cluster. As the cluster grows, the AA motif remains, but

part of the electron density is now delocalized over multiple water molecules. At $n\sim25$, there is a change of slope in both the VDEs (an observation not explicitly reported in a previous work [21]) and excited state lifetimes [285] of the isomer I cluster, providing further support for evolution of the electron binding motif in this size range. No abrupt changes in the IR-PD spectra are observed in the range from n=15 to n=50, supporting the notion of a gradual transition in the way the hydrogen-bonded water network binds the excess electron. Summarizing, vibrational spectroscopy yields important insight into the binding motif of the hydrated electron in finite clusters. However, it may be unable, in this particular case, to answer convincingly the question of internal vs. surface solvation, even when infrared spectra of larger water cluster anions become available.